This is the final draft of an article published in the Journal of Bridge Engineering. Volume 11, Issue 2, pp. 241-249 (March/April 2006), available at http://dx.doi.org/10.1061/(ASCE)1084-0702(2006)11:2(241)

The Effect of Vehicle Velocity on the Dynamic Amplification of a Vehicle crossing a Simply Supported Bridge

Sean P. Brady[1], Eugene J. OBrien[2], and Aleš Žnidarič[3]

[1]Texcel Pty Ltd, South Brisbane, Queensland, Australia.

Formally of Dept. of Civil Engineering, University College Dublin, Ireland

[2]Dept. of Civil Engineering, University College Dublin, Ireland

[3]Slovenian National Building and Civil Engineering Institute, Slovenia

CE Database Subject Headings: dynamic analysis, velocity, trucks, amplification

Abstract

Many authors, using both experimental tests and complex numerical models, have examined the effect of vehicle velocity on a highway bridge's dynamic amplification. Although these tests and models give valuable quantitative information on dynamic amplification, they give little insight into how amplification is affected by individual vehicle/bridge parameters. This paper uses relatively simple numerical models to investigate the effect of vehicle velocity on a bridge's dynamic amplification. A single vehicle crossing a simply supported bridge is modeled as a constant point force. A set of critical velocities are determined associated with peaks of dynamic amplification for all beams. The reasons for these large amplifications are discussed. A more complex finite element model, validated with field tests, is used to test the applicability of the conclusions obtained from the simple models to a realistic bridge/vehicle system.

1 Introduction

The Dynamic Amplification Factor (DAF) of a bridge is defined as the maximum total (dynamic plus static) load effect divided by the maximum static load effect. High dynamic amplifications in highway bridges are due to a combination of many factors. The main ones are bridge natural frequency, the frequencies associated with vehicle axle hop and body bounce, the damping capacity of the bridge, the damping of the vehicle's suspension, the bridge pavement and approach pavement evenness, and finally the vehicle's velocity (DIVINE 1997). Authors such as Olsson (1991) and Liu et al. (2002) found that a bridge's DAF is sensitive to the velocity of the crossing vehicle and Green et al. (1995) suggest that maximum amplification factors occur at different vehicle velocities for different bridges. A large number of authors such as Greco & Santini (2002), Fafard (1997) and DIVINE (1997) found that, as a crossing vehicle's velocity increases, the amplification factor of the bridge alternates between high and low DAFs. Although experimental work and complex finite element models can give valuable information regarding the magnitude and occurrence of these amplifications, they give little insight into the contribution of vehicle velocity to large DAFs. In this paper, the simple model of a single point force is used first to represent a single vehicle crossing a simply supported bridge. This model involves several significant simplifications. The mass of the vehicle is assumed to be small compared to the mass of the bridge. Only gravitational forces are considered. The vibration of the vehicle is ignored; therefore interaction between the vehicle and the bridge is also ignored. This model is clearly different from reality in many respects. It is developed here merely to gain an understanding of some of the principal factors which result in high amplification factors, namely bridge frequency, vehicle velocity and bridge

damping. The validity of the results is tested using a considerably more elaborate three-dimensional finite element model. The three-dimensional model is validated using field tests carried out on a bridge with two trucks in Slovenia. The results from the field tests are presented and discussed. In a companion paper (Brady & OBrien 2005), a two point force system is used to represent a 2-axle vehicle or two (uniaxial) vehicles traveling in the same or opposing directions.

2 The Dynamic Amplification Factor due to a Single Point Load

The case of a single vehicle crossing a simply supported bridge is modeled as a point force crossing a simply supported beam at a constant velocity. The modeling of the system is based on the work of Frýba (1971). The beam illustrated in Figure 1 is modeled using the Bernoulli-Euler differential equation:

$$EJ\frac{\partial^4 v(x,t)}{\partial x^4}+\mu\frac{\partial^2 v(x,t)}{\partial t^2}+2\mu\omega_b\frac{\partial v(x,t)}{\partial t}=\delta(x-ct)P \qquad (1)$$

where t is the time since the force arrived on the beam; $v(x,t)$ is the beam vertical deflection at point x and time t, measured from the equilibrium position when the beam is loaded with its self weight only; E is the modulus of elasticity; J is the 2nd moment of area (assumed constant), μ is the mass per meter, ω_b is the circular frequency of damping of the beam; P is a concentrated force of constant magnitude. $\delta(x)$ is the Dirac function and c is the constant velocity of the load. It is assumed that, initially (t=0), there is zero beam deflection and zero beam rotation. Damping is

assumed to be proportional to the velocity of motion of the beam. Equation 1 is solved using the method of integral transformations assuming modal superposition. The contribution of each mode j is summed to determine the bending moment response of the beam. The authors found that the solution converges satisfactorily when the first 20 modes of vibration are considered although fewer modes may be necessary to ensure convergence.

Using the model described, the dynamic amplification factors at mid-span for a simply supported beam being crossed by a point load were determined at various velocities. Figure 2 shows the contour plot of dynamic amplification factor as a function of load circular frequency ($\pi c/l$) and beam first circular frequency. For this figure 3% damping was assumed for the beam; this was considered to be reasonably typical (DIVINE 1997). A value of 13 rad/s (2.07 Hz) is taken as the minimum practical beam circular frequency. It is apparent from the figure that there are a number of ridges that represent local maximum dynamic amplification factors. For the case of zero damping, these ridges form a series of straight lines (Brady 2004). In addition, the magnitude along the top of each ridge is constant. As the level of beam damping increases in the system, there is a slight loss of linearity in these ridges. However, for practical purposes, this loss of linearity is negligible. Figure 3 shows the ridges representing local maximum dynamic amplification factors against beam first circular frequency and load circular frequency for three particular beams. Only the first four ridges are shown.

It can be concluded that a set of critical beam first circular to load circular frequency ratios exist. From these Critical Frequency Ratios the corresponding critical load

velocities, which produce local-maximum amplification factors, can be determined. Taking an average of the slopes of the line segments of each ridge in Figure 3 gives the Critical Frequency Ratios presented in Table 1.

2.1 Example

A 25m beam with a span to depth ratio of 20 and a rectangular solid cross-section with a width of 8.5 m is considered. The beam is assumed to be of concrete construction with a modulus of elasticity of 36×10^9 N/m^2 and a density of 2446 kg/m^3. These properties result in the beam having a first natural frequency of 3.47 Hz (21.9 rad/s). The damping value for the beam is assumed to be 3%. Figure 4 shows the relationship between dynamic amplification and load circular frequency. This figure corresponds to a horizontal section through Figure 2. The ridges illustrated in Figure 3 are clearly evident with DAF's of 1.01, 1.03, 1.08 and 1.39. The maximum dynamic amplification factor occurs at 8.37 rad/s (240 km/hr or 150 mph). The other high dynamic amplification factors occur at load circular frequencies of 3.23 rad/s, 2.02 rad/s, and 1.47 rad/s. To investigate why these high amplifications occur, it is helpful to examine the individual bending moment responses at each local maximum. Bending moment versus time responses for each of the Critical Frequency Ratios given in Table 1 (corresponding to critical vehicle speeds) are shown in Figure 5. The term 'normalized bending moment' refers to the total bending moment response divided by the mid-span static bending moment. In effect, the maximum value of the normalized bending moment response is the DAF.

The first local-maximum amplification factor occurs when the bending moment versus time response contains one peak. The second local-maximum occurs when the

response contains three peaks, the third corresponds to five peaks and the fourth has seven peaks. Therefore the maximum dynamic amplification factors occur when the bending moment response has an odd number of peaks. In addition, it is clear that each local-maximum amplification factor is governed by the magnitude of the central peak in the response (1^{st} of 1, 2^{nd} of 3, 3^{rd} of 5 and 4^{th} of 7).

It is interesting to consider the changes in dynamic amplification factor with respect to velocity. At high velocities the load reaches mid-span in less time than it takes the beam to vibrate once and the dynamic amplification factor is low (see right hand side of Figure 4). As the velocity falls, the dynamic amplification factor increases until it reaches a maximum at the Critical Frequency Ratio of 0.383; this response is illustrated in Figure 5. As the velocity decreases further, the magnitude of the single peak begins to decrease and a second peak begins to form in the response, corresponding to two beam vibrations. As the velocity continues to decrease, the second peak in the response increases and becomes higher than the first peak. A third smaller peak appears. This trend continues until the second peak reaches a maximum at the Critical Frequency Ratio of 0.148. With a further decrease in Frequency Ratio, a fourth peak begins to form and the pattern continues. This is the manner in which high amplification factors occur for all beams, with the velocities at which they occur clearly indicated by the Critical Frequency Ratios.

The effect of beam damping was investigated for a single load crossing a simply supported beam. It was found that the value of damping substantially affected the magnitude of the resultant amplification factors. As the level of damping in the beam

decreased the magnitude of the amplification factor increased. However, the Critical Frequency Ratios remain practically unchanged regardless of the level of damping. Thus for practical purposes, the Critical Frequency Ratios described in Table 1 are independent of the level of beam damping.

3 Experimental Dynamic Amplification Factors

An experiment was undertaken in Slovenia to investigate the dynamic amplification of a particular bridge. The results are used in two ways; firstly, the dynamic amplification factor for the bridge in question is determined. Secondly, the collected data is used to validate a finite element model. The experiment was carried out on April 20th, 1999 using two pre-weighed test vehicles. The test examined the dynamic amplification for single and pairs of vehicles crossing the bridge.

The bridge is a 32 m long, simply supported span that forms part of a larger multi-span structure. It has two lanes with bi-directional traffic flow and is slightly curved. The deck is of beam and slab construction. Figure 6 shows a schematic of the plan, cross-section, and details of the longitudinal beams and transverse diaphragm beams. Information regarding the depth of the asphalt pavement and the slab was not available; only the combined depth was recorded. Two pre-weighed vehicles were used in the test, one two-axle (2A) and one three-axle (3A), as shown in Figure 7. The axle spacings are 4.35 m for the two-axle vehicle and 3.22 m and 1.37 m (from the front) for the three-axle vehicle. The measured masses of the front and back axles of the two-axle vehicle are 3,460 kg and 12,900 kg respectively. The masses of the front

axle and rear tandem of the three-axle vehicle were 6,240 kg and 18,220 kg respectively.

A total of twelve strain transducers were placed on the underside of the bridge beams to measure strain data. The transducers were calibrated using the finite element results presented in section 4.2. Axle detectors were placed on the road surface to provide information on vehicle velocity and position. Photocells were placed on each vehicle, which, in conjunction with reflective strips placed on the bridge railings, gave additional information on vehicle velocity. Accelerometers were placed on all of the axles on the two-axle and three-axle vehicle. The data was recorded on a laptop using a scanning frequency of 512 Hz.

3.1 Experimental results

Frequency analysis was carried out on the strains from a transducer placed on the beam on the underside of the Lane 1, at mid-span. The analysis was carried out for 28 vehicle runs and the fundamental bridge frequency was determined to be 3.58 Hz (22.5 rad/s). The higher frequencies were determined as 4.60 Hz, 12 Hz and 13.02 Hz. Various free vibration signals were examined to determine the level of bridge damping. It was found to be between 2% and 4%. There was a high level of noise present in the vehicle accelerometer readings. The two-axle vehicle' frequencies were in the range of 2.1 Hz to 2.75 Hz and 11 Hz to 14 Hz. The frequency ranges of the three-axle vehicle were 2.1 Hz to 2.87 Hz and 9 Hz to 13.5 Hz.

The dynamic amplification factors for the two-axle and three-axle vehicles individually crossing the bridge are presented in Figure 8. It is clear that there is an insufficient number of vehicle crossing events to accurately determine the effect of vehicle velocity on the dynamic amplification. In general the dynamic amplification factor for the two-axle vehicle was higher than for the three-axle vehicle. The average values are 1.16 and 1.06 for the two- and three-axle vehicles respectively when the vehicle was in Lane 1. When the vehicle was in Lane 2, the average amplification factors were 1.29 and 1.14 for the two and three-axle vehicles respectively. The smaller factors for the three-axle vehicle may be due to the fact that it was significantly heavier than the two-axle vehicle. As the mass of a vehicle increases, its dynamic amplification factor decreases; this has been observed by many authors such as Kirkegaard et al. (1999), Huang et al. (1992) and DIVINE (1997). It is also clear that the amplification factor for the vehicles travelling in Lane 2 are higher than the amplification factors measured for Lane 1. The average amplification factors were 1.11 and 1.21 when the vehicles were in Lane 1 and Lane 2 respectively. This is due to the position of the strain transducer, which is situated almost directly underneath Lane 1. Zhu & Law (2002) concluded that, for a beam and slab bridge, the amplification factor for the beams directly underneath the vehicle is lower than for the beams further away from the vehicle. Huang et al. (1992) and Kirkegaard et al. (1999) also concluded that the amplification factor was lower for the lanes in which the vehicle was travelling than for the lanes in which the vehicle was not travelling.

It is clear from Figure 8 that the magnitude of the recorded dynamic amplification factors can vary considerably, even for the same vehicle velocity.. For example, for

the two-axle vehicle travelling in Lane 1 at approximately 30 km/hr, amplification factors of 1.09 and 1.25 were recorded. This may for a number of reasons, such as a change in the transverse position of the vehicle, a difference in road surface profile (due to a small change in the transverse position) or the vehicle vibrating differently as it enters the bridge.

The case of the two vehicles crossing the bridge simultaneously in opposing directions was also examined. Figure 9 shows the dynamic amplification factor for the two-vehicle event. The amplification factor is plotted against the velocity of the two-axle vehicle. In this figure, '3AL1 & 2AL2' and '2AL1 & 3AL2' mean three-axle vehicle in Lane 1 with two-axle vehicle in Lane 2, and two-axle vehicle in Lane 1 with three-axle in Lane 2. As in the case of the single vehicle crossing, there were an insufficient number of crossing events to determine accurately the relationship between the dynamic amplification factor and the velocity of the two vehicles. Likewise there was no clear pattern in the relationship between either vehicle's meeting position on the bridge. However, it is clear from the figure that the dynamic amplification factors for two vehicles on the bridge are considerably less than for a single vehicle. This has been observed by many other authors such as Zhu & Law (2002) and Kirkegaard et al. (1999).

4 Finite Element Analysis

The finite element (FE) program MSC/NASTRAN is used to construct the three-dimensional bridge and vehicle models used in the Slovenian experiment. These

models are validated using the experimental results and used to examine the effect of vehicle velocity on dynamic amplification. The bridge slab and footpaths are modeled as a series of plate elements, while the longitudinal beams and transverse diaphragms are modeled as offset beam elements - Figure 10.

The combined depth of the bridge slab and the asphalt pavement was measured on site. However, the individual depths are unknown. Various depths of asphalt and concrete were tested and the resultant model's natural frequencies compared to the measured bridge frequencies. An accurate bridge model could be achieved using a slab depth of 0.25 m and ignoring the mass of the asphalt surfacing (Brady 2004). The bridge is of concrete construction, but no information was available on its material properties. Following a frequency analysis, a modulus of elasticity of 4.8×10^{10} N/m^2 and Poissons Ratio of 0.15 was selected. This resulted in a first natural frequency of 3.54 Hz, considered a reasonable approximation of the experimental value of 3.58 Hz. The higher FE model frequencies of 4.66 Hz, 13.38 Hz and 13.92 Hz also showed good agreement with the measured values of 4.60 Hz, 12 Hz and 13.02 Hz. The level of damping in the bridge model was estimated at 3%.

The road surface is modeled as a random process described by the power spectral density (PSD) function given by Yang & Lin (1995) and implemented by González (2001). The road surface profile for the bridge is chosen as ‘Good’ with a roughness coefficient of 16×10^{-6} m^3/cycle (Wong, 1993). A 10 cm bump is incorporated to represent the expansion joint at the entrance to the bridge.

Vehicle models of both the two- and three-axle vehicles were constructed. The body of the vehicles are modeled as rigid frames and the suspension as spring and dashpot systems. Each vehicle's axles are modeled as rigid bars and each tire as a spring and dashpot system. A schematic of the two-axle vehicle model is shown in Figure 11. The three-axle vehicle is almost identical except that it has an additional axle. Mass elements are included in the model, just above each of the suspensions. The information regarding axle masses, vehicle inertial properties and suspension and tire parameters was obtained from experimental studies carried out in Munich (Baumgärtner 1998, Lutzenberger & Baumgärtner 1999) and on a Finnish instrumented truck (Huhtala 1999). Manufacturers information (Kirkegaard et al, 1999) was also considered. Further details of the vehicle parameters can be found in Brady (2004). The vehicle properties were adjusted so that the frequency ranges of both agreed with those found by experiment. The necessary adjustments were found to be minimal.

The interaction between the bridge and the vehicle is implemented using a Lagrange technique. Cifuentes (1989) first developed this method for the problem of a single circular moving mass crossing a one-dimensional beam. González (2001) extended the theory to allow for multiple wheel loads in three-dimensions. The Lagrange multiplier formulation defines a set of auxiliary functions. These are used to generate a compatibility condition that ensures that the vehicle wheels remain in contact with the bridge deck. Using this formulation, the interaction force between the wheel mass and the bridge can be quantified. In turn, both the force and moment acting at a particular bridge node can be determined using these auxiliary functions.

4.1 Validation of FE model

The completed models were compared to the results from the experiment, namely from the data recorded from the strain transducer placed at the mid-span of the beam underneath Lane 1. The transducer calibration factor was determined by scaling typical time histories to the FE model results. Figure 12 shows the comparison between the experimentally measured stress and the model stress for the two-axle and three-axle vehicles crossing the bridge and meeting at approximately the mid-span. As can be seen from the figure there is a reasonable match. The level of vibration is similar in each case and the period of oscillation of the model stress is the same as the measured value. Similar comparisons were carried out for faster velocities; the matches between the model and experimental stresses were again found to be consistently reasonable (Brady 2004).

4.2 Computer model calculations of dynamic amplification factor

A more comprehensive analysis of the effect of vehicle velocity on dynamic amplification for the experimental bridge can be undertaken using the finite element model. The dynamic amplification factor for a single vehicle crossing the bridge is determined by carrying out a number of simulations at a range of velocities. Authors such as Liu et al. (2002) conclude that a vehicle's approach length is an important consideration when examining dynamic amplification. A number of approach lengths were considered and a length of 100 m was found adequate for each vehicle to reach a steady state of vibration. Figure 13 shows the dynamic amplification factors for both

vehicles individually crossing the bridge in Lane 1, and crossing in the opposite direction in Lane 2.

It is clear from the figure that the dynamic amplification oscillates between high and low values as the velocity of the crossing increases. The two-axle vehicle traveling in Lane 2 generates a higher amplification factor (1.4 at 50 km/hr) than that vehicle in Lane 1 (1.25 at 50 km/hr). The maximum amplification factor for the three-axle vehicle in Lane 1 is 1.16 at 80 km/hr and is 1.22 at 80 km/hr when the vehicle is in Lane 2. Thus, the maximum amplification factors for each vehicle occur at different velocities. The dynamic amplification factor is generally higher for the two-axle vehicle than for the three-axle vehicle. In addition, the dynamic amplification factor is generally lower for the vehicles traveling in Lane 1 than in Lane 2.

The effect of a different road surface profile is examined in Figure 14 (a). The figure shows the resultant dynamic amplification factors for two different profiles, A and B. Both profiles have a roughness level of 'Good'. It is clear from the figure that the profile difference greatly affects the magnitude of the dynamic amplification factor. However, the maximum amplification factors occur at approximately the same velocities. In addition, the average amplification factor is the same for both pavements. Figure 14 (b) shows a comparison of stress between the two-axle vehicle crossing the bridge in Lane 1 at 50 km/hr where a large discrepancy exists between amplification factors. The general shape of the responses is similar, the discrepancy occurring due to a difference between the relative magnitudes of the individual peaks.

Figure 15 shows a comparison of the dynamic amplification factor for the two-axle vehicle model traveling in Lane 1 with the point load model described in section 2. From initial inspection the two curves appear to match very poorly, as would be expected. However, the underlying reasons for the corresponding peaks are similar. Figure 16 shows the stress responses for the critical velocities in the finite element model. For the velocities of 30 km/hr, 50 km/hr, 70 km/hr and 100 km/hr, the responses have 13, 9, 5, and 3 peaks respectively. These critical velocities can be converted to Frequency Ratios and compared to the peaks for the single point load. Table 2 shows the comparison of maximum dynamic amplification factors.

A number of conclusions can be drawn from the table and Figure 15. There is an approximate match in the velocities at which the maximum amplification factors occur despite the enormous difference in the models. However, the complex model is clearly missing some of these maxima. This may be a natural phenomenon or may be due to the large velocity increment chosen in the finite element analyses. What is important to note is that the manner in which these maximum amplification factors occur is the same, i.e., the number of peaks in each case is the same for the simple and complex models.

The rear axle of the NASTRAN two-axle vehicle was considerably larger than the front axle. In effect, the vehicle acted quite like a single sprung load. If the axle weights of the vehicle were more balanced, it would be expected that the similarity between the simple and complex models would be less. Finally it is important to consider the mass of the FE vehicle used in the above analysis. The vehicle mass to

bridge mass ratio for the two-axle vehicle is 3 %. Ichikawa et al. (2000) suggest that when the mass ratio is less than 10 %, the vehicle mass can be ignored. Therefore, for the two-axle vehicle considered, it is reasonable to assume that the mass will have little effect on the resultant dynamic amplification factors. It is possible that if the mass of the vehicle were larger, the simple model may not be able to predict the critical velocities as accurately.

5 Conclusions

For the case of single point load crossing a simply supported beam at a constant velocity, it was found that maximum dynamic amplifications occur at a number of Critical Frequency Ratios. For a given bridge, these Frequency Ratios imply a number of critical load velocities. The level of beam damping does not significantly affect the critical ratios. However, damping does affect the magnitude of the individual amplification factors.

The amplifications observed in the Slovenian Bridge confirmed many phenomena observed in the literature. It was found that in general, the amplification factor for two vehicles simultaneously crossing the bridge in opposing directions was considerably less than for a single vehicle.

An FE model was calibrated using experimental strain data recorded in the experiment. This validated model was then used to investigate the conclusions arrived at using the simple point load model. For the case of a single vehicle crossing the

bridge, the single point load model was found to reasonably predict the vehicle velocities at which maximum dynamic amplifications occur. Furthermore, the single point load model reasonably predicted the manner in which they occurred, i.e., the number of peaks in the stress record. However, the simple model was unable to accurately predict the magnitude of the amplification factors.

Appendix. References

Baumgärtner, W. (1998). "Bridge-Truck Interaction: Simulation, Measurements and Load Identification." *5th International Symposium on Heavy Vehicle Weights and Dimensions*, Maroochydore, Australia.

Brady, S. P. (2004). *The Influence of Vehicle Velocity on Dynamic Amplification of Highway Bridges.* PhD Thesis, Dept. of Civil Engineering, University College Dublin.

Brady, S. P. & OBrien E. J. (2005). "The Effect of Vehicle Velocity on the Dynamic Amplification of Two Vehicles crossing a Simply Supported Bridge." *Journal of Bridge Engineering*, ASCE. [Manuscript No. 022947]

Cifuentes, A. O. (1989). "Dynamic Response of a Beam Excited by a Moving mass." *Finite Element Analysis and Design 5*, Elsevier Science Publishers B. V., Amsterdam, 237-246.

DIVINE Programme, OECD (1997). *Dynamic Interaction of Heavy Vehicles with Roads and Bridges*. DIVINE Concluding Conference, Ottawa, Canada, June.

Fafard, M., Bennur, M. & Savard, M. (1997). "A General Multi-Axle Vehicle Model to Study the Bridge-Vehicle Interaction." *Engineering Computations*, 15(5), 491-508.

Frýba, L. (1971). *Vibration of Solids and Structures under Moving Loads*. Noordhoff International Publishing, Groningen, The Netherlands.

González , A. (2001). *Development of Accurate Methods of Weighing Trucks in Motion.* PhD. Thesis, Department of Civil Engineering, Trinity College, Dublin, Ireland.

Greco, A. & Santini, A. (2002). "Dynamic Response of a Flexural non-classically Damped Continuous Beam Under Moving Loadings." *Computers and Structures*, 80, 1945-1953.

Green, M. F., Cebon, D. & Cole, D. J. (1995). "Effects of Vehicle Suspension Design on Dynamics of Highway Bridges." *Journal of Structural Engineering*, 121(2), 272-282.

Huang, D. H., Wang, T. L. & Shahawy, M. (1992). "Impact Studies of Multigirder Concrete Bridges." *Journal of Structural Engineering*, 119(8), 2387-2402.

Huhtala, M. (1999). "Factors affecting Calibration Effectiveness." *Proceedings of the Final Symposium of the Project WAVE*, Ed. B. Jacob, Hermes Science Publications, Paris, 297-306.

Kirkegaard, P. H., Neilsen, S. R. K. & Enevoldsen, I. (1999). "Dynamic Vehicle Impact for Safety Assessment of Bridges." *2nd European Conference Weigh in Motion of Road Vehicles*, Lisbon, Sept. 1998, Eds. E.J. OBrien & B. Jacob, European Commission, 353-262.

Liu, C., Huang, D. & Wang, T. L. (2002). "Analytical dynamic impact study Based on Correlated Road Roughness." *Computers and Structures*, 80, 1639-1650.

Lutzenberger, S. & Baumgärtner, W. (1999). "Interaction of an Instrumented Truck Crossing Belleville Bridge." *Proceedings of the Final Symposium of the project WAVE*, Ed. B. Jacob, Hermes Science Publications, Paris, 239-240.

Olsson, M. (1991). "On the Fundamental Moving Load Problem." *Journal of Sound and Vibration*, 154(2), 299-307.

Wong, J. Y. (1993). *Theory of ground vehicles*, John Wiley and Sons, 376-385.

Yang, Y. B. & Lin, B. H. (1995). "Vehicle-Bridge Analysis by Dynamic Condensation Method." *Journal of Structural Engineering*, 121(11), 1636-1643.

Zhu, X. Q. & Law, S. S. (2002). "Dynamic Load on Continuous Multi-Lane Bridge Deck From Moving Vehicles." *Journal of Sound and Vibration*, 251(4), 697-716.

Appendix. Notation

E - Young's modulus of the beam,

J - moment of inertia of the beam cross section (assumed constant),

P - concentrated force of constant magnitude,

c - constant velocity of the point load,

j - mode number,

l - beam or bridge span,

t - time coordinate with the origin at the instant the force arrives on the beam,

x - horizontal distance coordinate with the origin at the left-hand end of the beam,

μ - mass per meter of the beam (assumed constant),

ω_b - circular frequency of damping of the beam,

$v(x,t)$ - beam vertical deflection at point x and time t, measured from the equilibrium position when the beam is loaded with its self weight only,

$\delta(x)$ - Dirac function (impulse, also known as delta function).

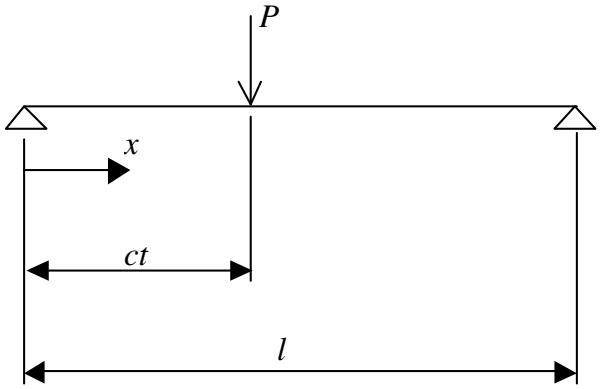

Figure 1 – Schematic of beam and load model

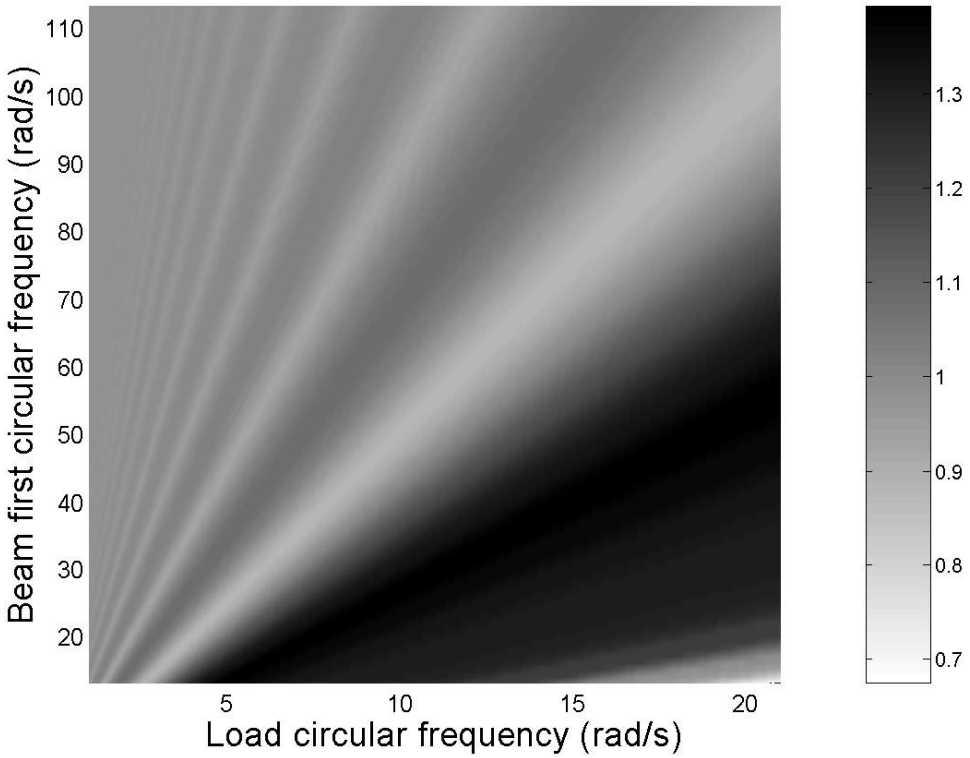

Figure 2 - Contour plot of amplification factor versus beam first circular frequency and load circular frequency (3 % damping)

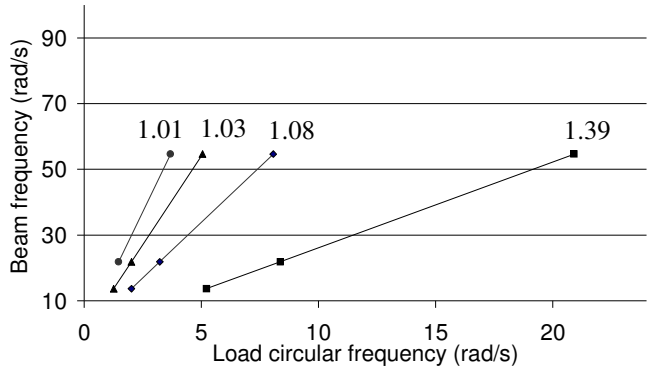

Figure 3 – Local maximum dynamic amplification factors with maximum value shown in each case (3% damping)

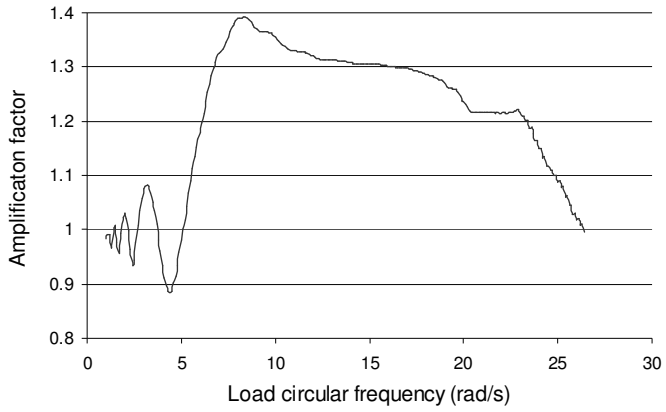

Figure 4 - Dynamic amplification factor versus load circular frequency for 25m bridge with 3% damping

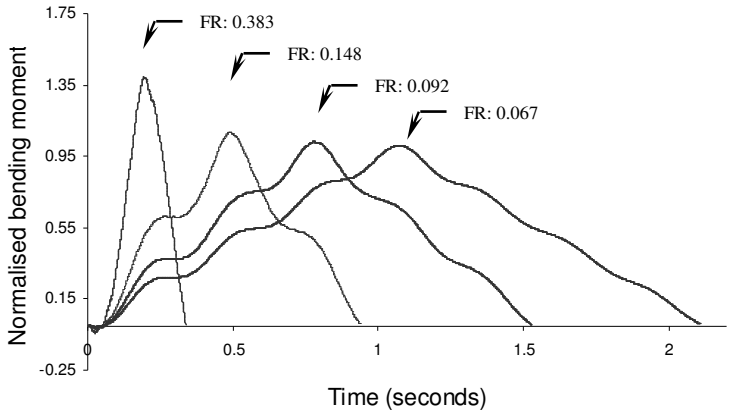

Figure 5 – Mid-span bending moment responses of 25m bridge with 3% damping

(FR = Frequency Ratio)

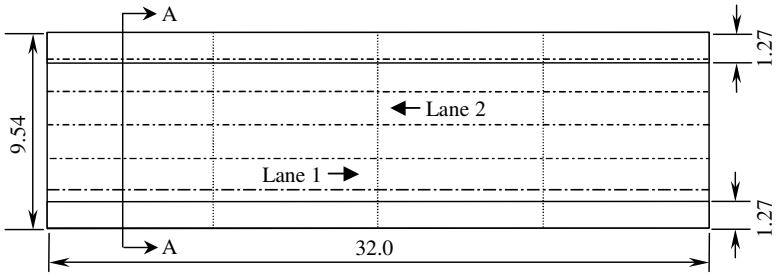

(a) – Plan, - - - - indicates center line of longitudinal beams and ..... indicates centerline of diaphragms

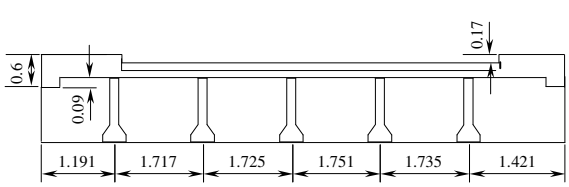

(b) – Section A-A

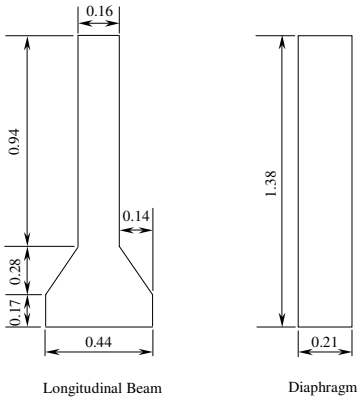

(c) - Longitudinal beam and transverse diaphragm

Figure 6 –Slovenian bridge details (all dimensions are in meters)

(a) – Two-axle vehicle

(b) – Three-axle vehicle

Figure 7 – Test vehicles

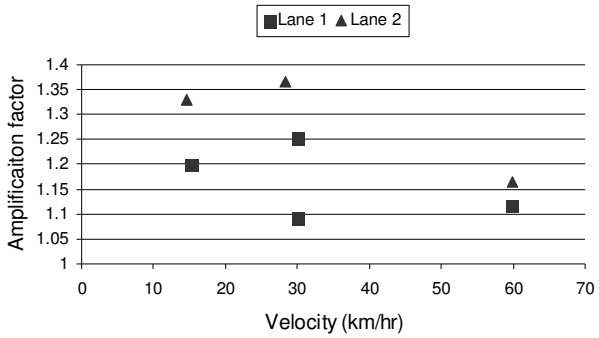

(a) - Two-axle vehicle

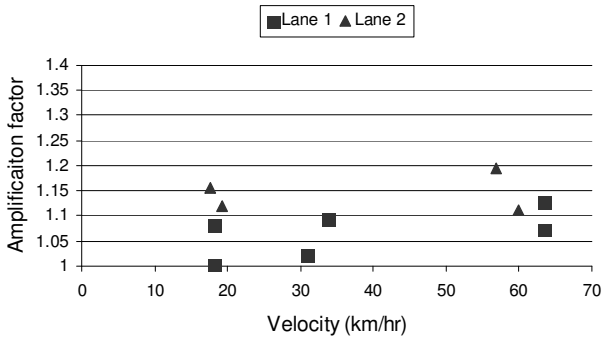

(b) - Three-axle vehicle

Figure 8 – Dynamic amplification factors for a transducer in Lane 1

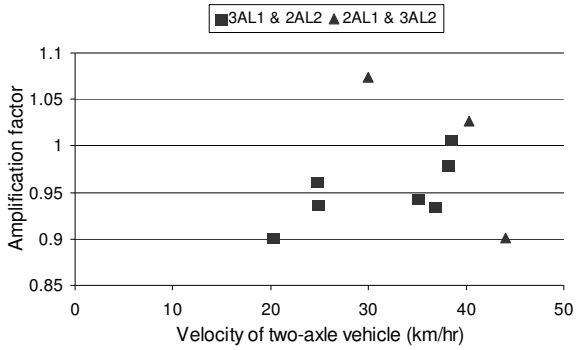

Figure 9 - Dynamic amplification factor for two vehicles

crossing bridge simultaneously

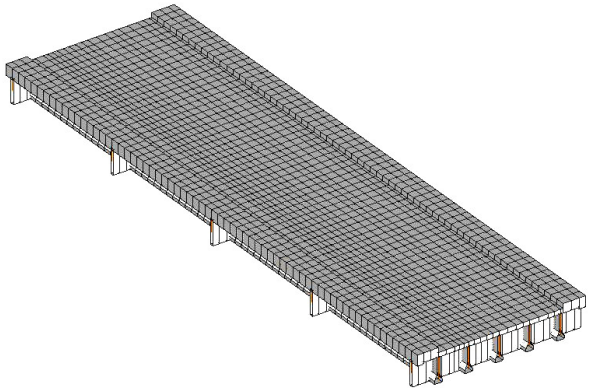

Figure 10 – Completed FE bridge model

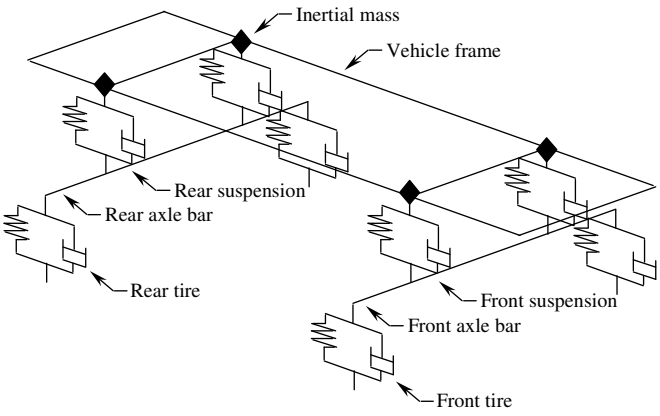

Figure 11 – Generic vehicle model (González , 2001)

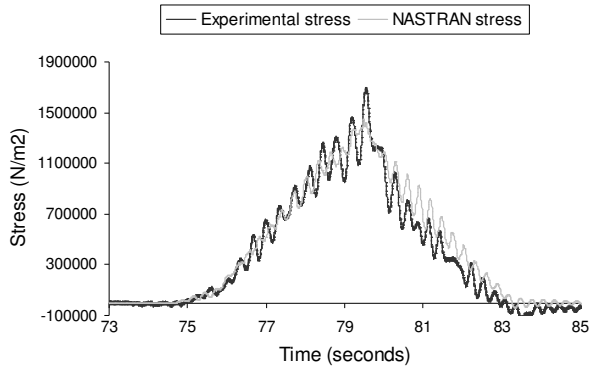

(a) - Two-axle vehicle traveling in Lane 1 at 15.16 km/hr

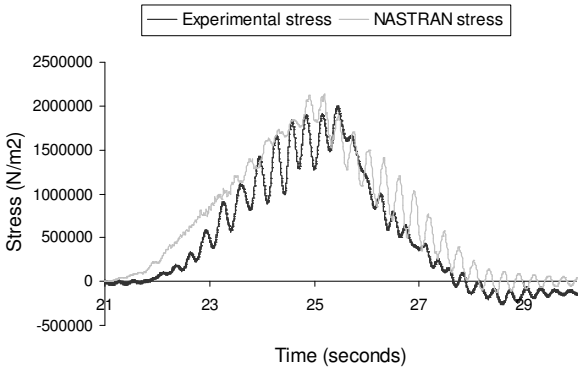

(b) - Three-axle vehicle traveling in Lane 1 at 17.93 km/hr

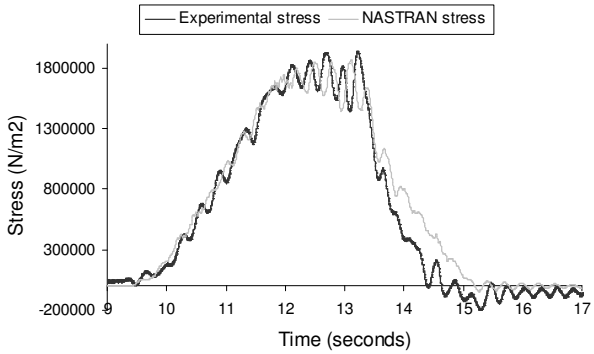

(c) – Two vehicle event

Figure 12 – Comparison of experimental and simulated vehicle crossing events

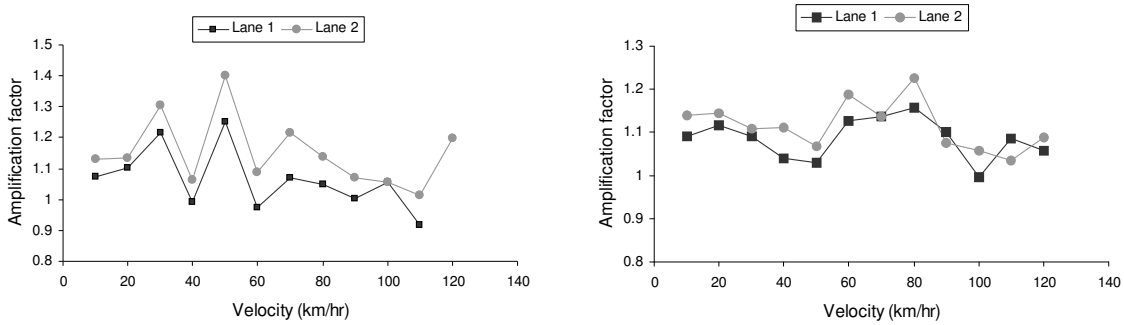

(a) - Two-axle vehicle (b) - Three-axle vehicle

Figure 13 – Dynamic amplification factor for vehicles crossing bridge

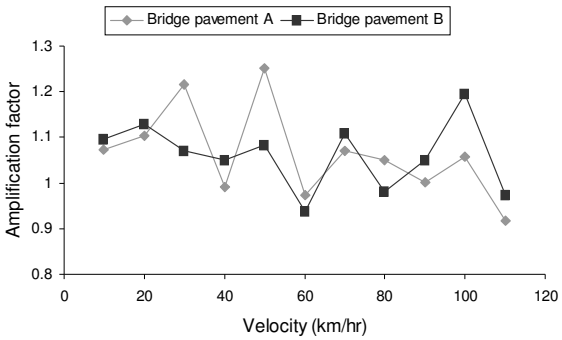

(a) - Effect of two different 'Good' pavement profiles

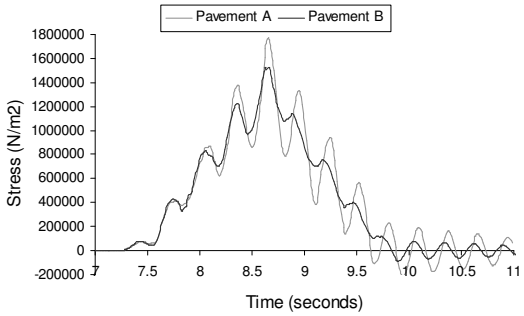

(b) - Effect of pavement profiles on dynamic response for two-axle vehicle in Lane 1

Figure 14 – Effect of pavement difference on dynamic amplification factor

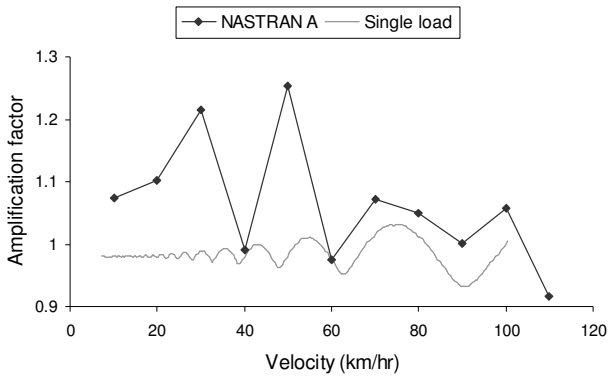

Figure 15 – Comparison of dynamic amplification factors for 32 m bridge for two-axle vehicle and point load

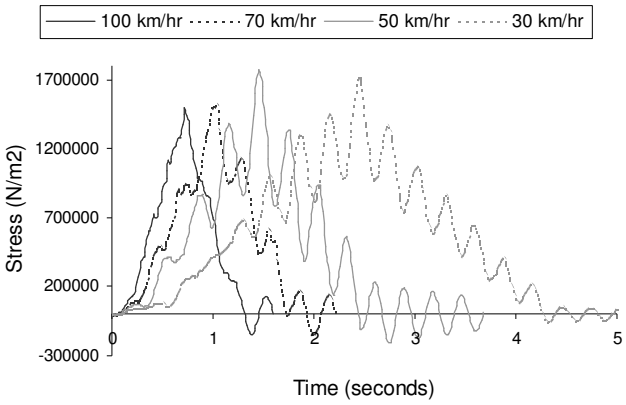

Figure 16 – Stress versus time responses for the critical vehicle velocities for two-axle vehicle model in Lane 1

Table 1 – The average Critical Frequency Ratios that produce local-maximum dynamic amplification factors for 3% damping

Frequency Ratio	Dynamic Amplification Factor
0.383	1.392
0.148	1.084
0.092	1.031
0.067	1.010

Table 2 – Comparison of maximum dynamic amplification factors (DAF)

Point load				Two-axle vehicle model			
Frequency Ratio	Velocity (km/hr)	No. peaks	DAF	Frequency Ratio	Velocity (km/hr)	No. peaks	DAF
0.3827	/	1	1.39	/	/	/	/
0.1477	120.61	3	1.08	0.1224	100	3	1.06
0.0924	75.49	5	1.03	0.0857	70	5	1.07
0.0675	55.09	7	1.01	0.0612	50	7	1.25
0.0530	43.27	9	1.00	/	/	/	/
0.0431	35.20	11	0.99	/	/	/	/
0.0368	30.07	13	0.99	0.0367	30	13	1.22
0.0323	26.40	15	0.98	/	/	/	/